

## Order-to-Chaos Transition in Rotational Nuclei

F. S. Stephens, M. A. Deleplanque, I. Y. Lee, A. O. Macchiavelli, D. Ward, P. Fallon, M. Cromaz, R. M. Clark, M. Descovich, R. M. Diamond, and E. Rodriguez-Vieitez

*Nuclear Science Division, Lawrence Berkeley National Laboratory, Berkeley, California 94720, USA*

(Received 3 May 2004; published 31 January 2005)

We have developed a new method to study the order-to-chaos transition in rotational nuclei. Correlations between successive  $\gamma$  rays are used to determine the average complexity of the intermediate levels and thereby the ratio of the interaction potential between levels to the level spacing. The measured ratios, 0.15 to 1.5, span the range from nearly fully ordered to nearly fully chaotic.

DOI: 10.1103/PhysRevLett.94.042501

PACS numbers: 21.10.Re, 23.20.Lv, 24.60.Lz, 27.70.+q

Chaos in quantal systems is not easily defined; however, a great deal of study has gone into comparing quantal systems with classical analogs, e.g., Sinai's billiard [1]. The result is some well established criteria for quantal systems that are thought to indicate whether the corresponding classical system would be ordered or chaotic. One of these is the so-called nearest neighbor distribution (NND), i.e., the distribution of energy separations between adjacent states having the same set of conserved quantum numbers (e.g., spin and parity). This method evaluates the fluctuations in the level spacings, which get smoothed out as a system becomes chaotic. The ordered levels are uncorrelated and thus have random energies which give exponentially decreasing numbers of energy spacings as the spacing size increases (Poisson). The smoothing can be understood as level repulsion arising from the mixing of states which eventually results in a skewed Gaussian NND (Wigner or GOE). It has been conjectured [1] that the Gaussian orthogonal ensemble (GOE) provides a complete description of quantal chaos in systems with time reversal symmetry. The mixing depends on the ratio,  $\nu/d$ , where  $\nu$  is the average interaction potential between the levels and  $d$  is their average energy separation. We believe this ratio can be measured directly and reliably in some rotational nuclei.

Early results in nuclei showed that near the neutron binding energy in a number of heavy nuclei ( $\sim 8$  MeV of excitation energy) the behavior is essentially chaotic [2], whereas, near the ground state in reasonably heavy deformed nuclei it is mainly ordered [3,4]. The Yb nuclei are in this region, and we study them using heavy-ion fusion reactions, which bring high angular momentum (up to  $\sim 70\hbar$ ) and excitation energy ( $\sim 80$  MeV) into the fused system. In these nuclei neutron evaporation quickly brings the average energy down to about the neutron binding energy, and the angular momentum and remaining energy are removed in a  $\gamma$ -ray cascade down to the ground state. We study this cascade which covers the range where chaos sets in. The Yb nuclei were chosen because nuclei in this region are deformed and exhibit rotational behavior. The  $\gamma$  rays in rotational cascades have correlations that are essential for this measurement.

The physics that generates nuclear  $\gamma$ -ray spectra in heavy nuclei is based on the motion of individual nucleons in the mean field generated by all the nucleons (e.g., Nilsson [5]). A residual interaction potential,  $\nu$ , is added, which is part of the nucleon-nucleon interaction that is not included in the mean field. In the Yb region, the mean-field states are ordered at very low temperatures [6], and as a result they each have distinctive rotational properties (emit a single  $\gamma$  ray of a characteristic energy), together with associated quantum numbers. With increasing excitation energy the separation between states,  $d$ , becomes small and the residual interaction mixes these states (compound damping) over an energy region whose width is called the spreading width,  $\Gamma_\mu$ . It is this mixing that generates the order-to-chaos transition we are discussing. The rotational properties are then also mixed (damped) so that each level now emits a spread of  $\gamma$  ray energies whose width is the rotational damping width,  $\Gamma_{\text{rot}}$  [7]. It has been recognized for some time that this rotational damping can provide an observable signal for the onset of chaos [6,8–10].

The relationship between these two types of damping is illustrated in Fig. 1. In the region of mixed levels a level (of spin,  $I$ ) with three components is shown on the right side of Fig. 1. Each of these components can emit a rotational  $\gamma$  ray with its characteristic energy. The level can then emit

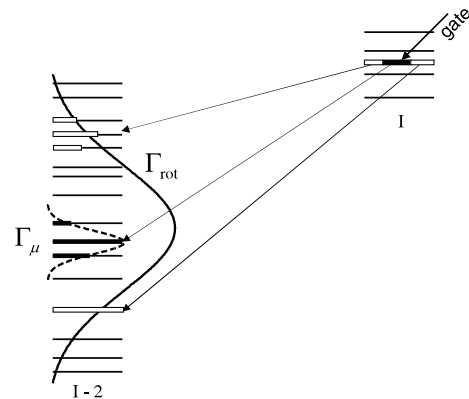


FIG. 1. A sketch of the mixed levels and transitions involved in rotational and compound damping. A gate is shown populating one component of a level having spin  $I$ .

any of these  $\gamma$  rays, which generates a distribution of  $\gamma$ -ray energies, whose width is  $\Gamma_{\text{rot}}$ . However, a new feature noticed by Matsuo [8] is that the compound damping can also show up in these spectra. This is illustrated on the left side of Fig. 1, where two of the components are schematically spread over three final states. The width of this distribution is  $\Gamma_{\mu}$ , which, in the nuclei and excitation-energy range we are discussing, is generally smaller than  $\Gamma_{\text{rot}}$ , as illustrated. It is also possible that the final state is unmixed as illustrated by the third component, and this results in a transition with a sharp (unspread) energy, characteristic of the well known discrete bands near the ground state. It would be difficult to separate these components in the full spectrum.

However, in a coincidence spectrum the first  $\gamma$  ray (the “gate”) will come in via one of the three components as illustrated in Fig. 1. The level can then decay via any of the components, but if it decays by the same (entry) component, it will have a narrow energy correlation with the gate transition characteristic of that component: either unspread (discrete) or spread only by the distribution of the final states,  $\Gamma_{\mu}$ . If it decays via either of the other two components, the width will be comparable to  $\Gamma_{\text{rot}}$ . Thus, if the components have equal amplitudes, the probability for the narrow structure,  $P_{\text{nar}}$ , will be one-third and that for  $\Gamma_{\text{rot}}$  will be two-thirds. This sensitivity to the complexity of the wave function suggests a connection between  $P_{\text{nar}}$  and chaotic behavior, and we want to explore that connection.

Our assumption is that  $P_{\text{nar}}$  is just  $c_a^2(a')$ , the square of the amplitude of the (unmixed) entry component,  $a$ , in the (mixed) decaying state,  $a'$ , and, since any component can be the initial component, we are measuring an average value. The spreading of the amplitude of an initial state,  $a$ , over an extended range of equally spaced levels has been treated [11] and leads to a Breit-Wigner distribution in energy for the strength,  $c_a^2(E)$ , with a width,  $\Gamma_{\mu}$ , given by Fermi’s golden rule. However,  $P_{\text{nar}}$  depends on the strength remaining in the initial state (at essentially the initial energy). This is related to the total strength lost to other states, but not specifically to the number of other states nor their energy distribution. With only the approximation that  $E_a \approx E_{a'}$ , we get

$$1/P_{\text{nar}} = 1/c_a^2(a') = 1 + (\pi v/d)^2. \quad (1)$$

Each measured value of  $P_{\text{nar}}$  depends on a single variable,  $v/d$ , and this is important since  $v/d$  is directly related to the chaotic behavior of a system.

To relate  $v/d$  to chaotic behavior we diagonalize a symmetric random matrix [12]. The diagonal elements are chosen randomly over an energy interval  $-E < 0 < E$  which defines both  $d$  and the initial NND (Poisson). The off-diagonal elements are chosen randomly from a Gaussian distribution centered at 0 and having an rms value,  $v$ . For any  $v/d$  this gives a set of levels from which standard measures of chaotic behavior can be evaluated.

For large  $v/d$  the behavior is chaotic with a Wigner NND. This model also gives a relationship between  $c_a^2(a')$  and  $v/d$ , where  $c_a^2(a')$  is the probability of the initial central state in the mixed central state. To get a good average value of  $c_a^2(a')$ , we made 500 diagonalizations of  $49 \times 49$  matrices for each  $v/d$  value, and this relationship is shown in Fig. 2 compared with that from Eq. (1). The agreement is good, giving us confidence that Eq. (1) and the random matrix are addressing the same problem.

The data were taken [13] using Gammasphere at the LBNL 88-Inch Cyclotron to record  $\gamma$  rays from the reaction of 215 MeV  $^{48}\text{Ca}$  projectiles on a 1 mg/cm<sup>2</sup> target of  $^{124}\text{Sn}$ . This reaction forms the fusion product,  $^{172}\text{Yb}$ , which decays into the product nuclei,  $^{168,167,166}\text{Yb}$ , with yields of roughly 20%, 40%, and 40%, respectively. Events were stored if five or more clean (no hit in the Compton suppressor)  $\gamma$  rays were in coincidence. About  $2 \times 10^9$  such events were recorded and sorted into a 2D ( $E_{\gamma}$ - $E_{\gamma}$ ) matrix. Correlation spectra were generated from the 2D matrix using the COR procedure [14] which subtracts an uncorrelated background from the data. For a gated spectrum this background is the full-projection spectrum normalized to the same area.

Our simulation generates the cascade of  $\gamma$  rays following the fusion reaction and has been previously described [13]. A very brief summary is given here. The cascade starts from a spin and an  $E^*$  ( $E^*$  is the excitation energy above the lowest energy level in the nucleus having that spin) randomly selected from distributions based on measured data. The cascade is a competition between  $E1$  statistical  $\gamma$  rays and  $E2$  rotational  $\gamma$  rays (whose properties were taken from measured data or from standard estimates [15]). Values for  $\Gamma_{\text{rot}}$  and  $\Gamma_{\mu}$  had the forms  $0.0033I(E^*)^{1/4}$  and  $0.029(E^*)^{3/2}$ , respectively. These values have the same functional form and coefficients within 10%–20% of those given in Ref. [7]. We used  $P_{\text{nar}}$  from Eq. (1), and in order to fit all the gates with a single simulation we took  $v/d$  proportional to  $(E^*)^{3/2}$  (the dependence expected in leading order, i.e., in mixing two-particle–two-hole states) and adjusted the coefficient to fit

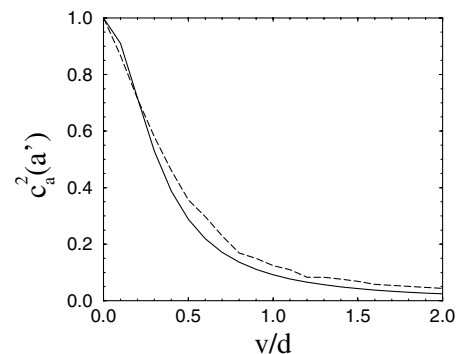


FIG. 2. The relationship of  $c_a^2(a')$  to  $v/d$  is shown for Eq. (1) (solid line) and the random matrix (dashed line).

the intensities of the narrow components. When  $E^*$  is less than 0.2 MeV we make the  $\gamma$  rays discrete, for which we randomly select a band from among the lowest two or three bands that are known to very high spins in each of the three Yb nuclei.

The data (black) and simulations (red) from this work are shown in Fig. 3 for eight gate energies. These spectra are all CORs and are what we call “shift-and-add” spectra: the gates cover a 60-keV range consisting of 15 4-keV wide channels. As each gate channel moves up or down, we move the coincident spectrum up or down by exactly the same amount. Thus the gate always occurs at the same channel in the coincident spectra, and we have 4-keV resolution for gate-related effects, whereas other effects tend to be smeared out. This is what we want.

For the higher-energy gates in Fig. 3 there is a broad peak that is a combination of the feeding and rotational correlations. This broad peak becomes smaller as the gate gets lower in the feeding region and actually becomes negative in the lowest two gates which are below all the feeding. In our previous work we called this negative correlation the secondary feeding correlation [13] and used it to get information about the feeding.

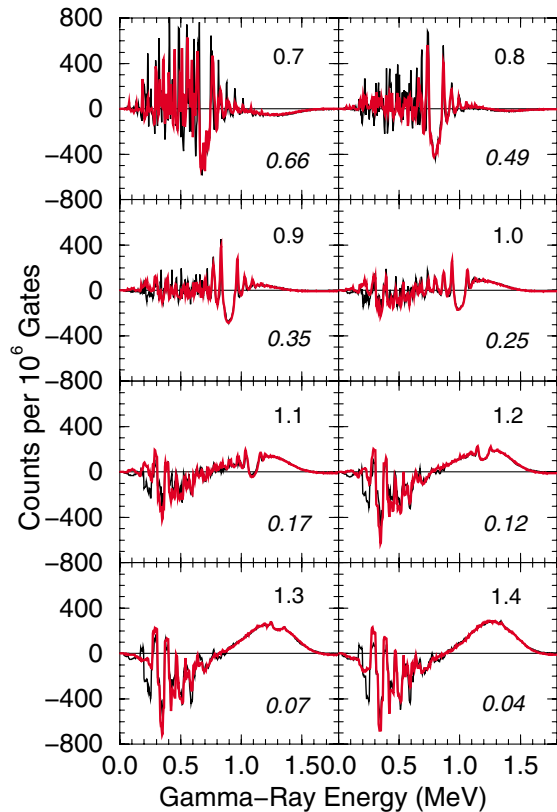


FIG. 3 (color). The data (black) and simulation (red) spectra (see text) are treated identically. The gate energy in MeV is at the upper right in each plot and the  $P_{\text{nar}}$  value is at the lower right.

Superposed on this broad feature is a narrow valley and ridge structure which gets progressively larger as the gate energy decreases. In detail this structure arises because a deexciting rotational band (discrete or compound damped) emits a regular set of  $\gamma$  rays (like a picket fence) and gating on one of these results in a spectrum missing this energy, i.e., with a valley. The transitions adjacent to the gate are seen as ridges which continue away from the gate energy as long as the population stays in the band and the  $\gamma$  rays are not smeared out in energy. This is what we have called the narrow structure whose intensity (roughly the area of the valley) indicates how much of the population enters and decays via the same component of the wave function. (Note that these structures can be easily resolved although, due to the high level density, individual  $\gamma$  rays above  $\sim 1$  MeV are largely unresolvable using present detectors.) Early studies of this narrow component showed it was a separate structure superposed on the rotational-damped spectrum and rough measurements of its intensity were made, in general agreement with the present values [16].

Measurements of  $P_{\text{nar}}$  are simple and reliable. They do not require identifying separately the compound-damped and discrete  $\gamma$  rays. Both of these  $\gamma$ -ray types arise from events that enter and decay via the same component of the wave function, and they produce similar valleys in the spectrum. Thus, measuring  $P_{\text{nar}}$  is much easier and more reliable than measuring  $\Gamma_{\mu}$ , for example, which does require identification of the above  $\gamma$ -ray types. In fact, measuring  $P_{\text{nar}}$  does not necessarily require the use of a simulation code. With the statistical  $\gamma$  rays subtracted and the spectrum unfolded to remove Compton-scattered  $\gamma$  rays,  $P_{\text{nar}}$  can be determined by integrating the area of the valley and comparing with the area corresponding to one transition as has been done [16]. We believe using a simulation is a more reliable way to determine  $P_{\text{nar}}$ .

To measure  $v/d$  we ensure that the simulation fits the data (e.g., Fig. 3) and then record for each gate the fraction of the rotational  $\gamma$  rays that make up the narrow component (i.e., the compound-damped and discrete  $\gamma$  rays). This is the average  $P_{\text{nar}}$ , and we then solve Eq. (1) for the average  $v/d$ . This can be done for any gate energy and width, and there is very little change with gate width up to 60 keV. Eight values of  $P_{\text{nar}}$  are given in Fig. 3, and a ninth value of 0.82 was measured for a 0.6 MeV gate. The uncertainties on these values are estimated to vary from  $\sim 10\%$  for the lowest gate (0.6 MeV) to  $\sim 30\%$  for the highest. All nine  $v/d$  values are given on Fig. 4 and the uncertainties corresponding to those on  $P_{\text{nar}}$  are all  $\sim 20\%$ . At very low energies ( $\leq 0.5$  MeV) the resolved discrete lines become strong, and we do not always reproduce these well because we include only two or three bands per nucleus. This should have little effect on our  $P_{\text{nar}}$  values. Another problem is that our simulation indicates there should be extensive motional narrowing [7], especially at the highest  $\gamma$ -ray energies. This would affect  $\Gamma_{\text{rot}}$  but

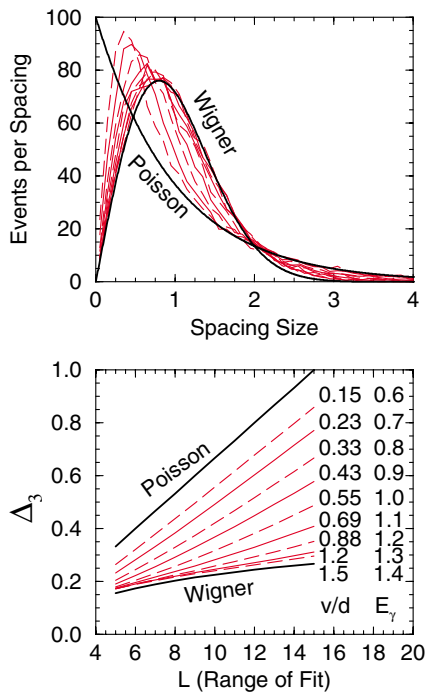


FIG. 4 (color online). The distributions, NND (upper) and  $\Delta_3$  (lower), for the measured  $v/d$  values (indicated) together with the Poisson and Wigner limits (heavy lines). Starting with the first gate alternate gates are dashed to help distinguish them.

should not affect  $P_{\text{nar}}$ , and we have not included motional narrowing in this simulation.

The random matrix described was diagonalized for our measured  $v/d$  values. The NND plots are shown in the upper part of Fig. 4, where the abscissa is in units of the average level spacing. The  $\Delta_3$  statistics of Dyson and Mehta [17] are shown in the lower part of the figure, where  $\Delta_3$  is a measure of the fluctuations over an energy region of length,  $L$ , also in units of the average level spacing. This latter plot shows most clearly that our measured points span the onset of chaotic behavior in these nuclei. The behavior becomes chaotic as  $v/d$  becomes  $\sim 1$  as has been pointed out [18]. Of course, a single average  $v/d$  value cannot give a complete description of the nuclear behavior: we cannot tell, for example, whether the spread in  $v/d$  values is small or large. Nor can we get details about the variation of  $\Delta_3$  with  $L$ —we see only the behavior given by the average  $v/d$  value. However, our procedure gives a simple and direct measure of the chaos-to-order transition along the average deexcitation pathways in these nuclei.

The average  $P_{\text{nar}}$  values have been discussed until now because they depend on the area of the valley which is unambiguously determined when the fit to the data in that region is good. The simulation can provide much more information although it is not generally so well determined. Additional results indicate that there is a large spread in  $E^*$  for the  $\gamma$  rays in each gate and thus a large spread in  $v/d$

values. It would be more meaningful to relate  $v/d$  to  $E^*$  and, since  $P_{\text{nar}}$  and  $v/d$  depend only on  $E^*$  in the simulation, there are analytic formulas for  $E^*$ :

$$E^* = 0.91[(1 - P_{\text{nar}})/P_{\text{nar}}]^{1/3} = 2.0(v/d)^{2/3}. \quad (2)$$

The coefficients in Eq. (2) come from fitting the present data. The average values for  $E^*$  vary from 0.5 to 2.6 MeV for our gates; however, they depend to some extent on the simulation and its inputs, resulting in uncertainties that are difficult to evaluate at present.

This is a new way to explore the order-to-chaos transition in nuclei. It looks directly at a property of the wave function rather than at level spacings and can often be used where measuring the energy-level spacings is not possible. There are some obvious ways to extend these measurements: studying other nuclei, using experimental tags to define more specific decay pathways, and/or developing the simulations to establish and improve their reliability. It would also be interesting to look for other correlated quantities (like our  $\gamma$ -ray energies) that could be exploited to provide information on chaotic behavior or other properties.

This work has been supported in part by the U.S. DOE under Contract No. DE-AC03-76SF00098. We thank Sven Åberg for helpful discussions on this subject.

- 
- [1] O. Bohigas *et al.*, Phys. Rev. Lett. **52**, 1 (1984).
  - [2] O. Bohigas *et al.*, in *Nuclear Data for Science and Technology*, edited by K.H. Böchhoff (Reidel, Dordrecht, 1983), p. 809.
  - [3] J.F. Shriner *et al.*, Z. Phys. A **338**, 309 (1991).
  - [4] J.D. Garrett *et al.*, Phys. Lett. B **392**, 24 (1997).
  - [5] S.G. Nilsson, Dan. Mat. Fys. Medd. **29**, No. 16, 1 (1955).
  - [6] S. Åberg, Prog. Part. Nucl. Phys. **28**, 11 (1992).
  - [7] B. Lauritzen, T. Døssing, and R.A. Broglia, Nucl. Phys. **A457**, 61 (1986).
  - [8] M. Matsuoka *et al.*, Phys. Lett. B **465**, 1 (1999); Nucl. Phys. **A649**, 379c (1999); **A557**, 211 (1993).
  - [9] B.R. Mottelson, Nucl. Phys. **A557**, 717c (1993).
  - [10] V. Zelevinsky, Annu. Rev. Nucl. Part. Sci. **46**, 237 (1996).
  - [11] A. Bohr and B.R. Mottelson, *Nuclear Structure* (Benjamin, New York, 1969), Vol. 1, p. 304.
  - [12] P. Persson and S. Åberg, Phys. Rev. E **52**, 148 (1995).
  - [13] F.S. Stephens *et al.*, Phys. Rev. Lett. **88**, 142501 (2002); in *Frontiers of Nuclear Structure*, edited by P. Fallon and R. Clark, AIP Conf. Proc. No. 656 (AIP, New York, 2002), p. 40.
  - [14] O. Andersen *et al.*, Phys. Rev. Lett. **43**, 687 (1979).
  - [15] T. Døssing and E. Vigezzi, Nucl. Phys. **A587**, 13 (1995).
  - [16] F.S. Stephens *et al.*, Phys. Rev. Lett. **58**, 2186 (1987); **57**, 2912 (1986).
  - [17] F.J. Dyson and M. Mehta, J. Math. Phys. (N.Y.) **4**, 701 (1963).
  - [18] S. Åberg, Phys. Rev. Lett. **64**, 3119 (1990); P. Jacquod and D. Shepelyansky, Phys. Rev. Lett. **79**, 1837 (1997).